water

MDPI

Article

Efficient Inactivation and Removal of a Harmful Marine Algae—*Heterosigma akashiwo*—By UV-Assisted Permanganate Oxidation

Jianwei Zeng [1,2], Xuegang Chen [1], Shidi Jin [1] and Jiajia Fan [2,*]

[1] Ocean College, Zhejiang University, Hangzhou 310058, China
[2] School of Life and Environmental Sciences, Hangzhou Normal University, Hangzhou 311121, China
* Correspondence: fanjiajia@hznu.edu.cn

Abstract: Harmful algal blooms (HABs) caused by *Heterosigma akashiwo* are occurring in coastal waters frequently, posing a great risk to marine environments and subsequent treatment processes like desalination. UV-assisted permanganate oxidation (UV/$KMnO_4$) is recognized as an innovative advanced oxidation process. This study investigated the inactivation and removal efficiencies of *H. akashiwo* cells by UV/$KMnO_4$. Algal cells were effectively disintegrated into fragments by UV/$KMnO_4$. Also, the degradation of photosynthetic pigments, membrane lipid peroxidation, and severe oxidative stress in algal cells was observed. The removal efficiency of algal cells reached 80.2% by 20 min of UV/$KMnO_4$ oxidation, with a $KMnO_4$ dosage of 5 mg L^{-1}. In addition, the residual algal cells could be completely removed by a subsequent self-settling process, without an additional coagulation procedure. The fragmentation of algal cells caused by UV/$KMnO_4$ may facilitate the formation of algal flocs, thereby improving the cell settleability. Furthermore, UV_{254} was significantly reduced by UV/$KMnO_4$, which is expected to reduce the formation of disinfection byproducts and membrane fouling. This study elucidates that UV/$KMnO_4$ can be a promising technique for the efficient treatment of harmful marine algae.

Keywords: harmful marine algae; cell removal; oxidative damage; self-settling; UV/$KMnO_4$ process

Citation: Zeng, J.; Chen, X.; Jin, S.; Fan, J. Efficient Inactivation and Removal of a Harmful Marine Algae—*Heterosigma akashiwo*—By UV-Assisted Permanganate Oxidation. *Water* **2023**, *15*, 3633. https://doi.org/10.3390/w15203633

Academic Editor: Reynaldo Patiño

Received: 20 September 2023
Revised: 12 October 2023
Accepted: 14 October 2023
Published: 17 October 2023

1. Introduction

The frequent occurrence of harmful algal blooms (HABs) has been a critical environmental issue worldwide [1,2]. HABs can trigger the massive death of farmed fish and shellfish, thus causing severe impacts on aquaculture industries, natural communities, marine ecosystems, and public health [3,4]. As a common species that can form HAB, the raphidophyte *Heterosigma akashiwo* widely distributes in many areas, such as the coastal waters of China, Japan, and America, due to its characteristics of wide salinity, light intensity, and temperature [5]. Given their capacity to survive in harsh environments like ballast tanks, *H. akashiwo* is also known as an invasive species that can migrate to other marine areas and expend pollution regions [6,7]. Additionally, when blooms occur, high algal biomass and the associated organic matters can cause significant operational problems to water treatments (e.g., desalination), including increased chemical consumption, severe membrane fouling, and a lower rate of water production [8,9]. Consequently, it is necessary to treat harmful algae such as *H. akashiwo*, especially in circumstances like ballast water management systems and seawater desalination processes.

Conventional technologies such as ultraviolet (UV) irradiation and coagulation have been generally applied to treat marine algae [10,11]. UV irradiation can degrade proteins and photosynthetic pigments of algal cells, potentially resulting in the cytoclasis of cells under a higher UV dosage [12]. Although UV irradiation is recognized as a green disinfection technology that can destroy algal DNA [12,13], the cells may reverse DNA damage by photoreactivation and dark repair mechanisms, thus achieving re-growth [11,13]. As for coagulation, its efficiency in

algal removal is relatively limited. For instance, aluminum sulfate coagulant only removed 79.3% of harmful algae (*Oscillatoria* sp.) from a water column [14], and the efficiency was only ~60% in *H. akashiwo* removal by modified clay [15]. In addition, the effectiveness of coagulation can be easily affected by the water quality, such as the salinity, temperature, and dissolved organic matters like humic acid [10,16]. Therefore, $KMnO_4$ pre-oxidation can be applied to enhance the efficiency of coagulation due to its capability to generate adsorptive products [17]. However, excessive oxidation may lead to the release of undesirable metabolites from algal cells [17]. Hence, it is necessary to develop alternative technologies in the efficient inactivation and removal of HAB species (e.g., *H. akashiwo*).

The UV/$KMnO_4$ process is known as an emerging technology that can enhance the oxidation of micropollutants and organic metals by producing hydroxyl radicals (•OH) and active manganese species (RMnS) [18,19]. As documented previously, •OH shows great efficiency in inactivating algal cells [20,21]. In addition, the in situ-formed manganese dioxide (MnO_2), as a reduced product of $KMnO_4$, is a good adsorbent for the removal of heavy metals and organic particulates [19,22]. A recent study reports that *Microcystis aeruginosa* (a common bule-green algae in freshwater) can be completely inactivated by UV/$KMnO_4$; after treatment, the *M. aeruginosa* cells were efficiently removed during the subsequent self-settling process without an additional coagulant, due to the in situ-formed MnO_2 [23]. To our best knowledge, the efficiency of UV/$KMnO_4$ in the treatment of marine algae (e.g., *H. akashiwo*) has not been reported. There are considerable discrepancies between *M. aeruginosa* and *H. akashiwo*. The former belongs to prokaryotic algae, while the latter is classified as eukaryotic algae [24,25]. *H. akashiwo* cells generally have larger sizes (from 10 μm to 17 μm) than *M. aeruginosa* cells (from 2 μm to 7 μm) [26,27]. Additionally, *H. akashiwo* cells contain a nucleus and Golgi apparatus, without a cell wall [28,29]. In contrast, in the absence of a nucleus and Golgi apparatus, there is a cell wall in *M. aeruginosa* cells [30]. Previous studies have reported that the variations between different algal species may significantly affect the treatment efficiency of various technologies, such as UV-B irradiation and chlorine oxidation [31,32].

This study aimed to investigate the feasibility of the UV/$KMnO_4$ process in treating *H. akashiwo*-laden water. The specific objectives of this research were as follows: (1) evaluate the efficiency of cell removal during the UV/$KMnO_4$ and following self-settling process; (2) assess the impacts of different factors on the removal efficiency of algal cells by UV/$KMnO_4$, such as the oxidant dose, reaction time, and interference of humic acid; and (3) investigate the cell inactivation mechanism by considering the cell morphology, photosynthesis pigment, and oxidative stress.

2. Materials and Methods

2.1. Materials and Reagents

The algal strain *H. akashiwo* (QT-072) was obtained from Microalgae Group, Key Laboratory of Marine Ecosystem Dynamics, Second Institute of Oceanography, Ministry of Natural Resources, Hangzhou, China. The strain was cultured in a modified and sterile f/2 medium [33] at 25 ± 1 °C with a cool fluorescent light flux (12 h: 12 h light–dark cycle, 25 μmol photos m^{-2} s^{-1}). The algal cultures were shaken daily to avoid cell adhesion and incubated to a high cell density (above 1.0×10^5 cells mL^{-1}); then, they were diluted by an f/2 medium to achieve a cell concentration of ~8.0×10^4 cells mL^{-1}. The diluted algal suspension was adjusted with 0.1 M sterile hydrochloride to pH 8.25 ± 0.05 for the following experiments. Analytical-grade chemicals and reagents were employed, and solutions were prepared using ultrapure water (synergy, Merck Millipore, Burlington, USA).

2.2. Experimental Reactor and Procedures

The photochemical experiments were performed in a photoreactor (JT-GHX-A, Jutong, Hangzhou, China) with a low-pressure mercury lamp (GHP 212T5L/4, Heraeus, Hanau, Germany) in a quartz sleeve placed in the center, as described previously [23], which was equipped with nine reaction quartz tubes. The UV intensity was determined to be

0.88 mW cm^{-2} by iodide/iodate chemical actinometry [34]. A thermostat was equipped to produce circulating water at 25 ± 1 °C to keep a constant temperature. The *H. akashiwo* samples were continuously stirred by a magnetic stirrer in the quartz tube. The $KMnO_4$ stock solution (2 g L^{-1}) was introduced to *H. akashiwo* cultures (50 mL for each sample) to attain a $KMnO_4$ concentration of 3, 5, and 7 mg L^{-1}, as desired. Subsequently, the algal cultures were exposed to UV irradiation immediately. The solo UV irradiation and solo $KMnO_4$ oxidation test was conducted in the same manner but in the absence of $KMnO_4$ or UV light, respectively. The *H. akashiwo* samples were collected at specific time intervals and quenched immediately with sodium thiosulfate for analyses, including the cell density, photosynthetic pigments, the hemolysis rate, the ultraviolet absorbance at 254 nm (UV_{254}) of filtered *H. akashiwo* samples, and the activities of antioxidant enzymes, except for the determination of $KMnO_4$ residuals, the observation of the cell morphology, and algal self-settling tests. Three replicates were conducted for each treatment.

2.3. Cell Removal

For the treatment experiments (detailed in Section 2.2), samples with a volume of 2 mL were collected from a bulk sample for the measurement of cell density after exposure to UV alone, $KMnO_4$ alone (5 mg L^{-1}), and UV/$KMnO_4$ treatment (5 mg L^{-1}) for 5, 10, 15, 20, and 30 min. The residual treated algal culture (48 mL) was kept in the quartz tube and allowed to settle quietly. Samples were collected at a depth of 2 cm below the surface at each interval (30, 60, 120, and 240 min) to evaluate the cell removal efficiency during the self-settling process. In addition, the impacts of oxidant dosages (3, 5, and 7 mg L^{-1}) and humic acid (0, 5, and 10 mg L^{-1}) on the performance of $KMnO_4$ alone and UV/$KMnO_4$ treatments in cell removal during treatments and followed self-settling was assessed by adjusting one parameter at a time from the baseline condition (reaction time = 20 min, $[KMnO_4]_0$ = 5 mg L^{-1}). The removal efficiency of algal cells during treatments (R_t) and self-settling (R_s) was calculated by Equations (1) and (2), respectively:

$$R_t = (N_0 - N_t)/N_0 \times 100\% \quad (1)$$

$$R_s = (N_0 - N_s)/N_0 \times 100\% \quad (2)$$

where R_t (%) = the removal efficiency of algal cells during UV alone, $KMnO_4$ alone, or UV/$KMnO_4$ treatment; N_0 (cells mL^{-1}) = the initial cell density of *H. akashiwo* cells in the suspension; N_t (cells mL^{-1}) = the cell density of *H. akashiwo* at a given exposure time by UV alone, $KMnO_4$ alone, or UV/$KMnO_4$ treatment; R_s (%) = the removal efficiency of treated algal cells during the subsequent self-settling process; and N_s (cells mL^{-1}) = the cell density of *H. akashiwo* at a given settling time, respectively.

2.4. Analytical Methods

After a predetermined treatment time, the fresh algal suspension was immediately sampled for observation using microscopy (ECLIPSE E100, Nikon, Tokyo, Japan). Algal cells were formed as flocs in some samples during UV/$KMnO_4$ treatment. Therefore, the algal samples containing large flocs were dispersed using pipette aspiration/injection for the determination of cell density, according to a previous study [35]. Algal suspensions (2 mL for each sample) intended for algal enumeration were preserved with Lugol's iodine and subsequently examined under a microscope (Nikon ECLIPSE E100, Tokyo, Japan) at 100× magnification [36]. In addition, the concentration of Ca^{2+} in the f/2 medium was determined using inductively coupled plasma mass spectroscopy (ICP-MS, PerkinElmer, NexIon 350D, Waltham, MA, USA).

The algal samples (10 mL each) for the detection of the residual $KMnO_4$ concentration were filtered with 0.45 μm nylon filer (Jinteng, Tianjin, China) and then measured in a 5 cm quartz cuvette by a UV/VIS spectrometer (754, Jinghua, Shanghai, China) at a wavelength of 525 nm. UV_{254} could represent the content of double-bond and aromatic structures of organic matters [37]. Thus, an algal suspension with a volume of 10 mL was filtered with

a 0.45 μm glass-fiber membrane (Xinya, Shanghai, China) and then determined in a 1 cm quartz cuvette by a UV/VIS spectrometer (754, Jinghua, Shanghai, China) to obtain the UV_{254} value of the filtrate.

To obtain changes in chlorophyll-a and carotenoids during UV alone, $KMnO_4$ alone, and UV/$KMnO_4$ treatments, samples were extracted using a 95% ethanol solution at 4 °C for 24 h. The absorbance was measured at wavelengths of 470, 649, and 665 nm in a 1 cm quartz cuvette using a UV/VIS spectrometer (754, Jinghua, Shanghai, China). The contents of chlorophyll-a and carotenoids were calculated by referring to previous studies [38,39]. The algal culture (20 mL) was filtered with a 0.22 μm glass fiber filter (Xinya, Shanghai, China), and the filtrate was used for extracellular hemolytic toxin analysis using the erythrocyte lysis assay method, which was described previously by Chen et al. (2021) [40].

The malondialdehyde (MDA) is recognized as a product of lipid peroxidation, indicating the oxidative damage of algal cell membranes [41]. Oxidative stress was evaluated through measurements of enzyme activities in *H. akashiwo*, including catalase (CAT) and superoxide dismutase (SOD). The algal cells after treatments were collected by centrifugation (8000 rpm, 4 °C, 10 min) from a 40 mL algal suspension and then suspended in phosphate buffer solution (0.05 mol L^{-1}, pH = 7.8, volume = 8 mL). The cells were then disrupted by an ultrasonic cell crusher (JY92-IIN, Ningbo Scientiz, Ningbo, China) for 5 min with a 2 s pause after each 2 s pulse in an ice bath. The supernatant of the homogenate was collected by centrifugation (10,000 rpm) at 4 °C for 10 min and then stored at 4 °C for determining MDA, SOD, and CAT, according to a previous study [31]. The Bradford method was employed to determine the total soluble protein content in algal cells, which served as the basis for calculating MDA, SOD, and CAT activities [42].

3. Results

3.1. Algal Cell Morphology and Removal during UV/$KMnO_4$ Treatment

The morphological features of *H. akashiwo* cells after UV alone, $KMnO_4$ alone (5 mg L^{-1}), and UV/$KMnO_4$ treatments (5 mg L^{-1}) are shown in Figure 1. The algal cells in the control samples exhibited a clear sphere shape, with an intact cell structure (Figure 1a). The morphology of most algal cells was similar to that of the control during 30 min of UV irradiation (Figure 1b–d). However, many of the algal cells were ruptured after 30 min of $KMnO_4$ oxidation, with an irregular shape and lighter green color (Figure 1g). For UV/$KMnO_4$ treatment, the cytoclasis of algal cells was observed after only 10 min, and some cells were disintegrated severely into fragments (Figure 1h). Large algal flocs were formed after UV/$KMnO_4$ treatment for 20 min, with a size of ~250 μm in width and ~450 μm in length (Figure 1i). Even larger algal flocs were observed after 30 min, with a size of ~450 μm in width and ~750 μm in length (Figure 1j).

Figure 2 shows the removal efficiencies of algal cells (R_t) by UV alone, $KMnO_4$ alone, and UV/$KMnO_4$ treatments. In this study, some algal cells were seriously disintegrated into fragments during treatments, leading to a decrease in algal cell density, which was considered as cell removal. The R_t in UV alone and $KMnO_4$ (5 mg L^{-1}) alone was 36.8% and 28.9% after 30 min, respectively (Figure 2). The UV/$KMnO_4$ (5 mg L^{-1}) showed higher efficiency in algal removal, with an R_t of 77.8% after 30 min. The impacts of the initial $KMnO_4$ dosages and the addition of humic acid on *H. akashiwo* cell removal by $KMnO_4$ alone and UV/$KMnO_4$ treatments were also investigated. In general, the increasing $KMnO_4$ dosage promoted algal removal, and this phenomenon was more obvious during the UV/$KMnO_4$ process (Figure 3a). For instance, the R_t was increased from 13.6% to 43.7% by $KMnO_4$ alone, with a dosage from 3 to 7 mg L^{-1}, whereas it was increased from 22.2% to 86.5% in the UV/$KMnO_4$ process. The addition of humic acid significantly alleviated the removal of algal cells by $KMnO_4$ alone and UV/$KMnO_4$ treatments (Figure 3b). For instance, the R_t was decreased from 36.3% to 2.2% (in $KMnO_4$ alone) and from 80.2% to 21.3% (in UV/$KMnO_4$), respectively, with the addition of 5 mg L^{-1} humic acid (Figure 3b).

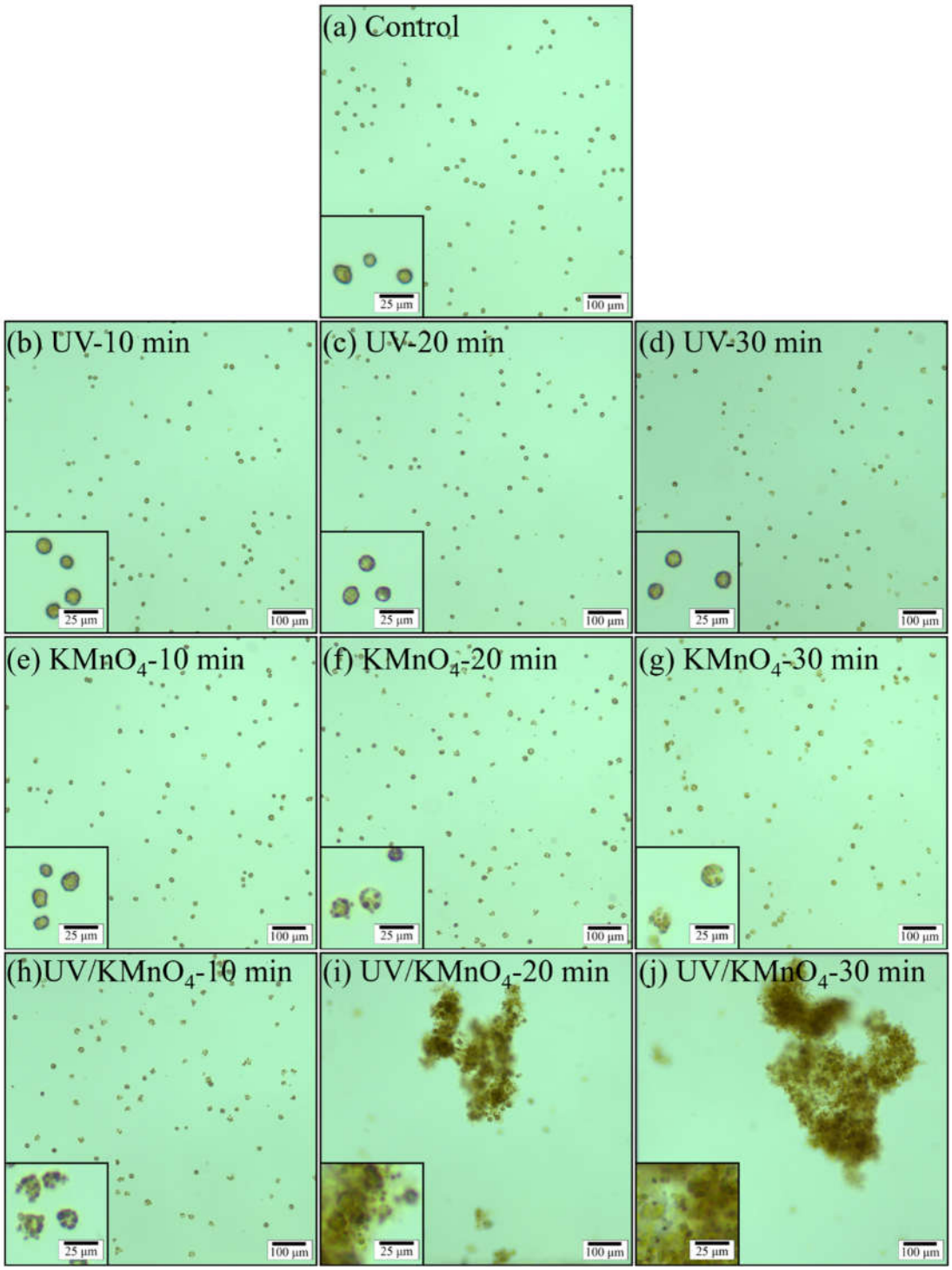

Figure 1. Optical microscopic images (main figure ×100, inserted figure ×400) of *H. akashiwo* cells during UV, $KMnO_4$, and UV/$KMnO_4$ treatments at different sampling times: (**a**) control; (**b**–**d**) UV irradiation; (**e**–**g**) $KMnO_4$ oxidation; and (**h**–**j**) UV/$KMnO_4$ oxidation. Conditions: $[KMnO_4]_0$ = 5 mg L^{-1}, exposure time = 10 min, 20 min, and 30 min.

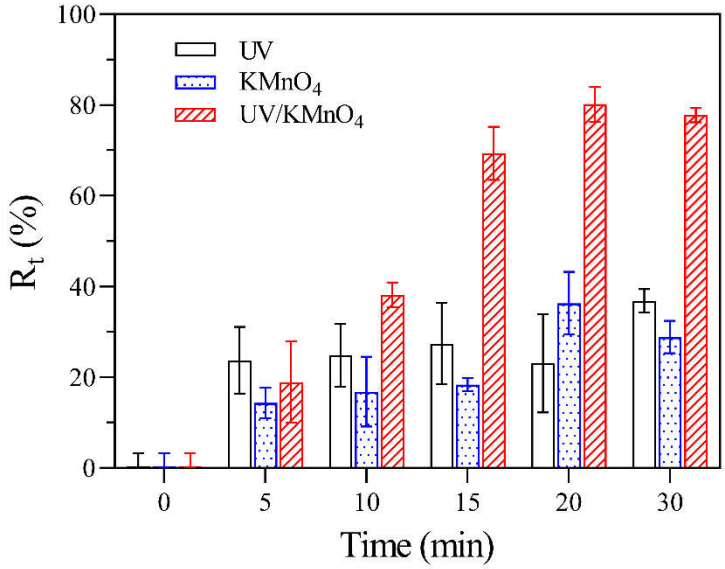

Figure 2. The R_t of *H. akashiwo* samples after UV, $KMnO_4$, and UV/$KMnO_4$ treatments at various exposure times. Conditions: $[KMnO_4]_0$ = 5 mg L^{-1}, exposure time = 0–30 min.

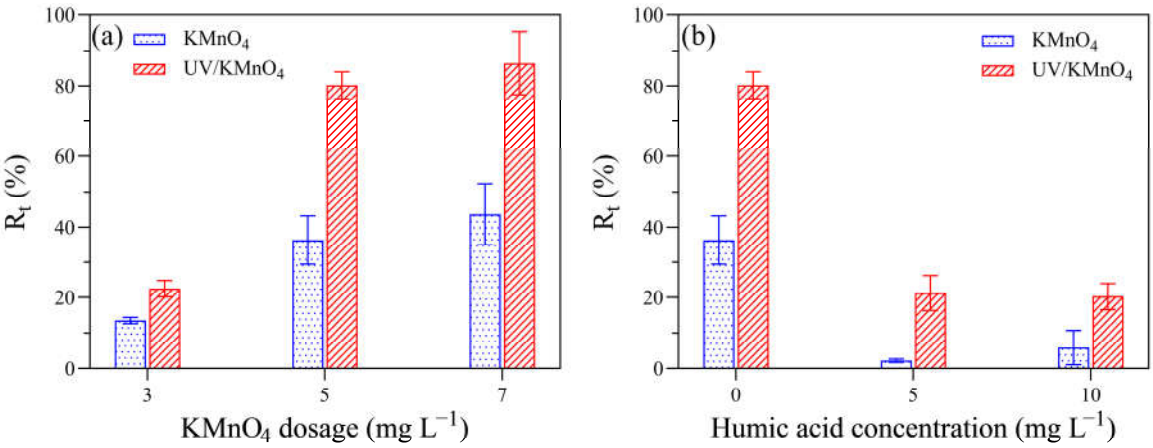

Figure 3. The impacts of various factors on the R_t of algal samples treated with $KMnO_4$ and UV/$KMnO_4$: (**a**) $[KMnO_4]_0$ = 3–7 mg L^{-1}, exposure time = 20 min; and (**b**) $[KMnO_4]_0$ = 5 mg L^{-1}, exposure time = 20 min, [humic acid]$_0$ = 0–10 mg L^{-1}.

3.2. $KMnO_4$ Decay

The decay curve of $KMnO_4$ was measured in the absence of algal cells to determine the oxidant demand of the background f/2 medium. For $KMnO_4$ alone, the concentrations of $KMnO_4$ decreased rapidly to 2.34, 4.15, and 5.96 mg L^{-1} in the first 5 min, with initial dosages of 3, 5, and 7 mg L^{-1}, respectively, while they remained almost constant in the following reaction time (Figure 4a). The decay pattern of $KMnO_4$ during the UV/$KMnO_4$ treatment was different, with a consistent decrease trend. The residual $KMnO_4$ concentrations in the UV/$KMnO_4$ treatment were 0.42, 1.89, and 3.19 mg L^{-1} after 60 min, where, respectively, 3, 5, and 7 mg L^{-1} of $KMnO_4$ were added initially (Figure 4a). The concentrations of $KMnO_4$ decayed more rapidly with the presence of *H. akashiwo* cells in both the $KMnO_4$-alone and UV/$KMnO_4$ treatments (Figure 4b). Only 0.22 and 0.47 mg L^{-1} of $KMnO_4$ were detectable in the algal samples treated by $KMnO_4$ alone for 30 min, and there is no $KMnO_4$ residual in the UV/$KMnO_4$ process, with initial $KMnO_4$ dosages of 3 and 5 mg L^{-1}, respectively (Figure 4b). A pseudo first-order kinetics model was used to estimate the rate constants (k_{decay}) of $KMnO_4$ decay, according to Equation (3):

$$C = C_0 e^{-k_{decay} t} \quad (3)$$

where C (mg L^{-1}) = residual $KMnO_4$ concentration after a certain exposure time; C_0 (mg L^{-1}) = $KMnO_4$ concentration at the initial time; k_{decay} (min^{-1}) = rate constants of $KMnO_4$ decay; and t (min) = the exposure time of various treatments. The k_{decay} was 0.088–0.179 and 0.105–0.690 min^{-1} in $KMnO_4$ alone and UV/$KMnO_4$, respectively (Table S1).

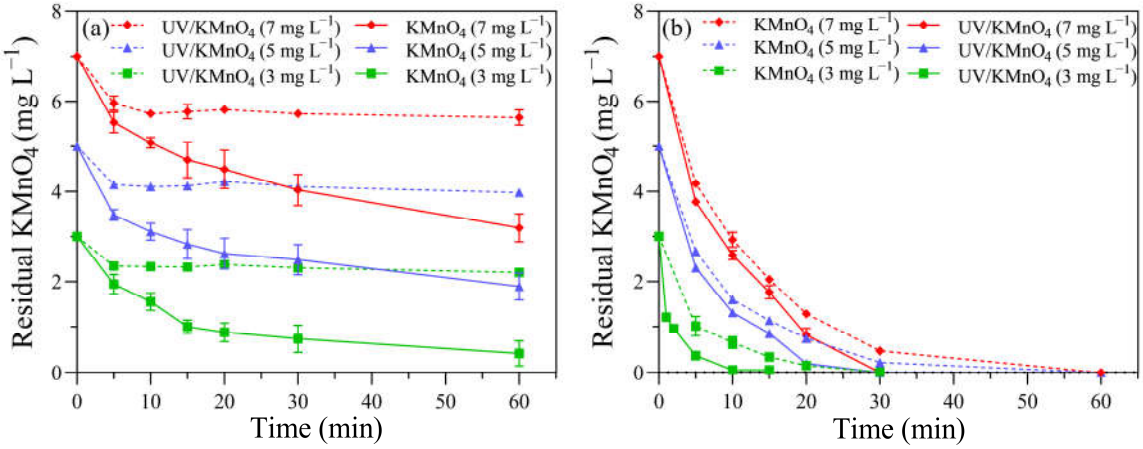

Figure 4. The $KMnO_4$ residual in samples treated with $KMnO_4$ and UV/$KMnO_4$: (**a**) without *H. akashiwo* cells and (**b**) with *H. akashiwo* cells.

3.3. The Change in the UV_{254} and Hemolysis Rate

Prior to treatments, the UV_{254} value of the algal filtrate was 0.139 cm^{-1} (Figure S1a). It increased to 0.154 cm^{-1} after 5 mg L^{-1} $KMnO_4$ oxidation for 30 min, while UV alone resulted in a slight decrease in the UV_{254}, with a value of 0.119 cm^{-1}. Compared to $KMnO_4$ alone or UV alone, a significant reduction in the UV_{254} value was observed in the UV/$KMnO_4$ (5 mg L^{-1}) process, i.e., the UV_{254} value was 0.062 cm^{-1} after 30 min of contact. The initial hemolysis rate in the algal filtrate was 1.3%. It increased to 3.8% and 4.0% in the $KMnO_4$ (5 mg L^{-1}) and UV/$KMnO_4$ (5 mg L^{-1}) treatments after 30 min, respectively, while a more significant increase in the hemolysis rate (7.8%) was induced by UV alone (Figure S1b).

3.4. Content of Photosynthetic Pigments and Antioxidant System Activity

Several physiological and biochemical characteristics of *H. akashiwo* cells were monitored. The initial concentrations of chlorophyll-a and carotenoids were 0.82 and 0.28 mg L^{-1}, respectively. There were 0.56, 0.67, and 0.63 mg L^{-1} of chlorophyll-a remaining after UV alone, $KMnO_4$ (5 mg L^{-1}) alone, and UV/$KMnO_4$ (5 mg L^{-1}) treatments for 30 min, respectively (Figure 5a). The concentrations of the remaining carotenoids were almost the same (~0.24 mg L^{-1}) after the three treatments (Figure 5b). The contents of the total soluble protein in the algal samples decreased with an increasing exposure time after all the treatments (Figure 6a). About 44.6% and 47.5% of the total soluble protein were decreased by UV alone and 5 mg L^{-1} $KMnO_4$ alone after 30 min, respectively, while a larger reduction (62.0%) was achieved by UV/$KMnO_4$ (5 mg L^{-1}) treatment. Compared to the initial value, the SOD activity in the algal samples increased by 391.7% with $KMnO_4$ treatment for 5 min, and it kept relatively constant during the remaining time (Figure 6b). The SOD activity remained constant during the first 15 min under UV irradiation, while it increased by 579.2% after 30 min. In contrast, the SOD activity of algal cells treated by UV/$KMnO_4$ treatment gradually increased by 1270.8% during the first 20 min, whereas it dropped subsequently (Figure 6b). The change tendency of the CAT activity of algal cells was similar to that of the SOD activity by all the treatments (Figure 6c). The largest increase in the MDA level was detected in algal cells by UV/$KMnO_4$ treatment (Figure 6d). For instance, the MDA level increased by 25.0%, 129.2%, and 275.0% after 30 min of the UV-alone, $KMnO_4$-alone, and UV/$KMnO_4$ treatments, respectively.

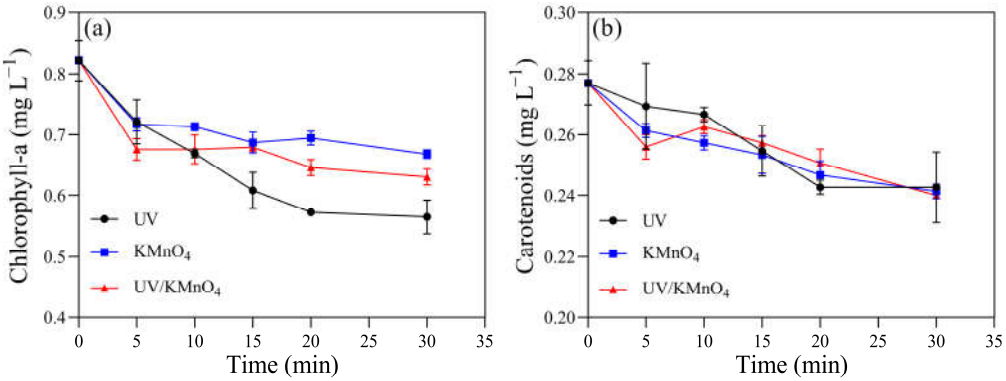

Figure 5. The contents of photosynthetic pigments in *H. akashiwo* samples treated with UV, $KMnO_4$, and UV/$KMnO_4$: (**a**) chlorophyll-a and (**b**) carotenoids. Conditions: $[KMnO_4]_0$ = 5 mg L^{-1}, exposure time = 0–30 min.

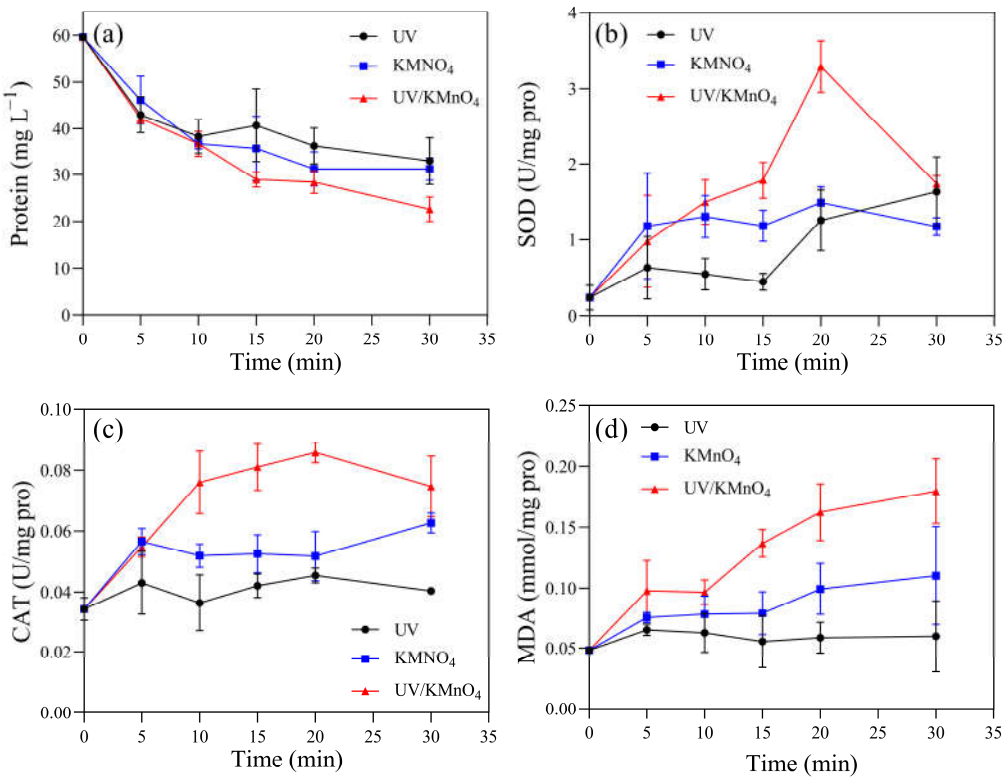

Figure 6. The contents of (**a**) total soluble protein, (**b**) SOD, (**c**) CAT, and (**d**) MDA in the *H akashiwo* samples treated with UV, $KMnO_4$, and UV/$KMnO_4$. Conditions: $[KMnO_4]_0$ = 5 mg L^{-1}, exposure time = 0–30 min.

3.5. Removal Efficiency of Algal Cells via a Settling Test

After the UV-alone, $KMnO_4$-alone, and UV/$KMnO_4$ treatments, the removal efficiency of residual algal cells in the suspension via subsequent self-settling (R_s) was investigated. Due to the high motility of *H. akashiwo*, approximately 20% of algal cells swam beyond the sampling range. Both $KMnO_4$ alone and UV/$KMnO_4$ facilitated algal removal during the following self-settling, while UV alone was inefficient (Figure S2). Therefore, the detailed self-settling tests were conducted only based on $KMnO_4$ alone and UV/$KMnO_4$ to assess the effects of the exposure time, dosages of $KMnO_4$, and contents of humic acid on the removal efficiency of algal cells (Figure 7). The exposure time of $KMnO_4$ alone had a minor impact on subsequent cell removal via self-settling. For example, after $KMnO_4$ treatment for 10 and 30 min, the R_s increased to around 66% within 60 min, and then it kept constant

during the remaining time (Figure 7a). Contrarily, the cell removal during the self-settling process was significantly affected by the pre-exposure time of the UV/$KMnO_4$ treatment. For instance, the R_s was 55.4% and 99.4% after 240 min of self-settling, with pre-exposure of UV/$KMnO_4$ for 10 and 30 min, respectively (Figure 7b). It is noteworthy that the R_s via self-settling after UV/$KMnO_4$ treatment is considerably higher than that in $KMnO_4$ alone, with the same $KMnO_4$ dosages (Figure 7c,d). The addition of humic acid (5–10 mg L^{-1}) led to decreases in R_s during the first 30 min of self-settling, after both $KMnO_4$-alone and UV/$KMnO_4$ treatments (Figure 7e,f). However, the R_s increased to similar values to those of samples without humic acid after 240 min of self-settling (Figure 7e,f).

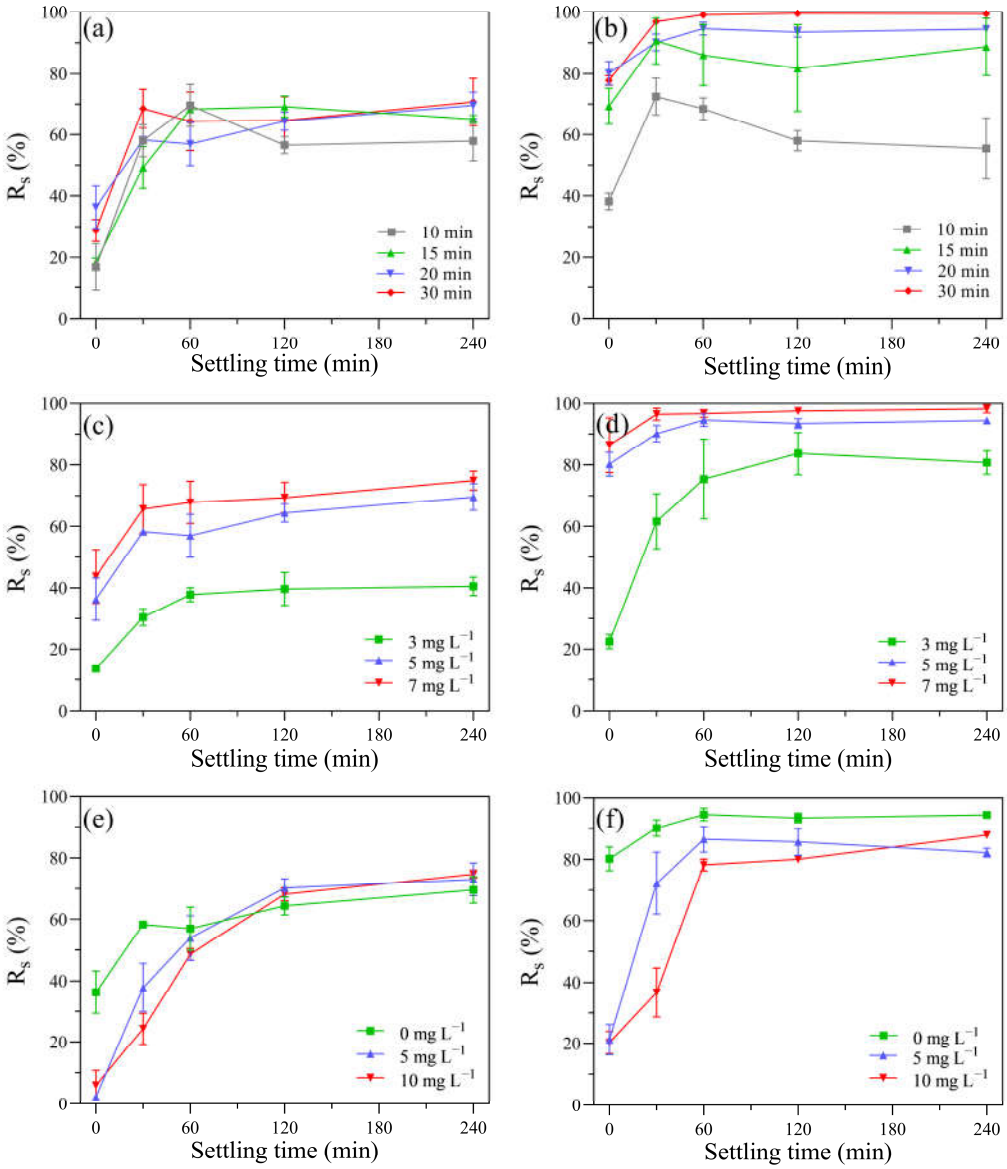

Figure 7. The impacts of various factors on the R_s of algal samples during the self-settling process in: (**a**) after $KMnO_4$ treatments ($[KMnO_4]_0$ = 5 mg L^{-1}, exposure time = 10–30 min); (**b**) after UV/$KMnO_4$ treatments ($[KMnO_4]_0$ = 5 mg L^{-1}, exposure time = 10–30 min); (**c**) after $KMnO_4$ treatments ($[KMnO_4]_0$ = 3–7 mg L^{-1}, exposure time = 20 min); (**d**) after UV/$KMnO_4$ treatments ($[KMnO_4]_0$ = 3–7 mg L^{-1}, exposure time = 20 min); (**e**) addition of humic acid in $KMnO_4$ treatments ($[KMnO_4]_0$ = 5 mg L^{-1}, exposure time = 20 min, $[humic\ acid]_0$ = 5–10 mg L^{-1}); (**f**) addition of humic acid in UV/$KMnO_4$ treatments ($[KMnO_4]_0$ = 5 mg L^{-1}, exposure time = 20 min, $[humic\ acid]_0$ = 5–10 mg L^{-1}).

4. Discussion

4.1. The Inactivation of H. akashiwo Cells by UV/KMnO$_4$

UV/KMnO$_4$ treatment significantly improved the disruption of *H. akashiwo* cells, compared to UV alone and KMnO$_4$ alone (Figure 1). Previous studies have indicated KMnO$_4$ is a relatively moderate oxidant for algae treatment [36,43,44]. For instance, only 2.5% of *M. aeruginosa* cells were lysed after 20 mg L^{-1} KMnO$_4$ treatment for 2 h [45]. However, this study showed that *H. akashiwo* was very sensitive to KMnO$_4$ (5 mg L^{-1}) oxidation, with 36.3% of the cells lysed in 20 min (Figure 2). It is likely that there is no cell wall in *H. akashiwo* cells to protect them [29]. This agrees with previous studies showing that different species of algae may have varied responses to the same treatment process, due to different cellular characteristics [31,32,46]. UV/KMnO$_4$ resulted in a severer disruption of *H. akashiwo* cells (Figure 1h–j), probably due to the generation of HO• [18,19]. HO• has a high redox potential (E_0 = 2.8 V) and can damage algal cells by the destruction of proteins, lipids, and DNA [47]. A recent study also showed that a species of freshwater algae (*M. aeruginosa*) can be efficiently ruptured by UV/KMnO$_4$ [23]. Therefore, it suggests that UV/KMnO$_4$ can be a promising method in damaging both of freshwater and marine algae.

In addition to causing cell disruption, the photosynthetic and antioxidant enzyme systems of *H. akashiwo* were also damaged by UV/KMnO$_4$ (Figures 5 and 6). The total soluble protein, as an essential component of microorganisms, is one of the indicators reflecting cell metabolism activity [48]. The results showed that UV/KMnO$_4$ treatment caused the largest decrease in the total soluble protein (Figure 6a), suggesting it severely disrupted the metabolic activities of algal cells. However, serving as light-harvesting pigments and an energy transfer medium in photosystems [44,49], the contents of chlorophyll-a and carotenoids in algal cells only decreased slightly by all the treatments (Figure 5). This agrees with previous studies indicating that chlorophyll-a and carotenoids were more resistant to UV radiation or oxidation, compared to protein [12,50]. This study also assessed the activities of two important intracellular antioxidant enzymes (SOD and CAT) in algal cells (Figure 6). They can protect cells from excess reactive oxygen species (ROS) and alleviate oxidative damage. For instance, SOD catalyzes the dismutation of O_2•$^-$ to H_2O_2, and then H_2O_2 can be further degraded to water and molecular oxygen by CAT [51]. The SOD and CAT activities of algal cells by UV/KMnO$_4$ treatment were increased remarkably during the first 20 min (Figure 6a,b), indicating that the antioxidant enzyme defense system was activated to resist the attack of ROSs induced by UV/KMnO$_4$ [52]. However, both the SOD and CAT levels declined subsequently (Figure 6b,c), which suggested that ROS induced by UV/KMnO$_4$ may exceed the antioxidant capacity and cause damage to the antioxidant enzyme defense system [25]. The significant increase in the MDA content also implied that algal cells were severely damaged by the UV/KMnO$_4$ treatment (Figure 7d), since MDA is a major product of lipid peroxidation in algal cell membranes [41]. These results are consistent with the phenomena observed from the optical microscopic images (Figure 1), confirming that the efficient inactivation of *H. akashiwo* cells was achieved by UV/KMnO$_4$ treatment.

4.2. The Impacts of UV/KMnO$_4$ Treatment on Water Quality

This study found that the decay of KMnO$_4$ in an algal suspension was faster than that in an f/2 medium, for both KMnO$_4$-alone and UV/KMnO$_4$ treatments. This may be due to the fact that algal cells and their associated organic matters can readily react with KMnO$_4$ [53,54]. The concentration of KMnO$_4$ decreased more rapidly in the UV/KMnO$_4$ treatment than in KMnO$_4$ alone (Table S1; Figure 4). A residual of 0.45 mg L^{-1} was detected after KMnO$_4$ oxidation for 30 min (Figure 4b), which would result in a pink color ($\geq$0.05 mg L^{-1}) in the treated water [43]. However, the complete decomposition of KMnO$_4$ was achieved in the UV/KMnO$_4$ process (Figure 4b). This may be attributed to the fact that UV irradiation can facilitate the decomposition of MnO_4^- to MnO_2 [55]. Previous studies have also reported that KMnO$_4$ is rapidly reduced to insoluble MnO_2 during the UV/KMnO$_4$ process [18,23]. The final product, MnO_2, can be easily removed in the subsequent process, avoiding the color problem for treated water.

UV_{254} is regarded as an indicator for evaluating membrane fouling and disinfection byproducts (DBP) formation potential, as it exhibits a positive correlation with both of them [37,56]. The surface-adsorbed organic matter can be desorbed from the algae cell surface by $KMnO_4$ alone [57]. In addition, $KmnO_4$ alone can induce algal cell lysis and the release of intracellular organic matter [26], leading to an increase in the UV_{254} value. Compared to $KMnO_4$ alone and UV alone, a greater reduction in UV_{254} was observed in the algal samples treated by UV/$KMnO_4$ (Figure S1a). This may be attributed to the formation of HO• and RMnS in the UV/$KMnO_4$ process, which have high reactivity toward organic matter containing double bonds and benzene rings [58,59]. This result suggests that the UV/$KMnO_4$ process may alleviate membrane fouling and reduce DBP formation potential, thus enhancing the efficiency of water treatment (e.g., desalination) and ensuring the treated water quality.

The initial homolysis rate in the algal filtrate was relatively low in this study (Figure S1). This was consistent with a previous study that demonstrated that there are usually a small number of dissolved hemolytic toxins in healthy *H. akashiwo* cells [40,60,61]. The hemolysis rates in the algal filtrates only increased slightly after all the treatments, while UV alone resulted in the highest release of hemolytic toxins (Figure S1b). According to the results, the algal cells were disrupted into fragments (Figure 1), and thus, the release of intracellular toxins may occur in the UV/$KMnO_4$ process; however, the increase in hemolytic toxins was minimal (Figure S1b). It is possibly because the released hemolytic toxins were rapidly oxidized by the UV/$KMnO_4$ process at the same time [43,44,52]. Therefore, those phenomena indicate that UV/$KMnO_4$ treatment can effectively inactivate algal cells, without posing negative impacts on water quality.

4.3. Algal Cell Removal during the UV/$KMnO_4$ and Subsequent Self-Settling Processes

Compared with UV alone and $KMnO_4$ alone, UV/$KMnO_4$ caused more significant damage to algal cells, thus resulting in efficient cell removal (R_t) (Figure 2). In addition, the R_t was improved with the $KMnO_4$ dosage increasing from 3 mg L^{-1} to 7 mg L^{-1} (Figure 3a). Humic acid is a major fraction of the dissolved organic matters in source waters, which may reduce the efficiency of water treatment processes [46]. As shown in Figure 3b, the addition of humic acid decreased the efficiency of algal removal during both $KMnO_4$-alone and UV/$KmnO_4$ treatments. The reduced efficiency may be attributed to the consumption of the oxidant by humic acid [46]. Additionally, humic acid has been proven to have an inner-filter effect that may reduce the incident UV light intensity [62]. However, the R_t in UV/$KMnO_4$ was still higher than that in $KMnO_4$ alone. The higher efficiency achieved by UV/$KMnO_4$ may be attributed to the generation of HO• and RMnS, which oxidized humic acid and thus reduced the interference [58,63].

Higher efficiencies in algal cell removal (R_s) were observed during subsequent self-settling after the $KMnO_4$-alone and UV/$KMnO_4$ treatments, compared to UV alone (Figure S2). This may be attributed to the in situ-formed MnO_2 from the $KMnO_4$ reduction, which could promote the aggregation and settleability of algal cells by coating their surface and increasing the specific gravity [23,26,64]. The R_s after UV/$KMnO_4$ treatment was considerably higher than that after $KMnO_4$ alone (Figure 7a,b). One possible reason for this is that the UV/$KMnO_4$ treatment was more effective in disintegrating algal cells into fragments (Figure 1). The fragmentation of algal cells may reduce the steric hindrance and enhance the collision and attachment between the algal cells and fragments, thus achieving the formation of large flocs [65]. In addition, larger amounts of in situ MnO_2 can be generated in the UV/$KMnO_4$ process than in $KMnO_4$ alone, which was conducive to the aggregation and removal of algal cells [23].

As a common factor affecting Al coagulation, humic acid could reduce the cell removal efficiency and increase the dosage of coagulants [16]. Although the R_s was decreased by the presence of humic acid during the first 60 min of self-settling, it gradually increased during the followed settling time and achieved a similar value with the algal samples without humic acid conditions (Figure 7e,f). This may be attributed to the high concentration of

calcium ions (Ca^{2+}) in the background water (f/2 medium; 334 mg L^{-1} as Ca^{2+}). Previous studies have reported that Ca^{2+} has a cation bridging effect in promoting the aggregation of MnO_2, humic acid, and algal cells, therefore facilitating the removal of algal cells [64,66]. The concentration of Ca^{2+} in seawater is approximately 400 mg L^{-1} [67], which would benefit algal removal. Therefore, the results indicate that algal cells in the seawater can be efficiently removed by UV/$KMnO_4$.

5. Conclusions

The combination of $KMnO_4$ and UV irradiation in the treatment of the harmful marine algae *H. akashiwo* was investigated for the first time. The UV/$KMnO_4$ treatment effectively inactivated *H. akashiwo* cells by disrupting their cellular structure, inducing oxidative stress, and disturbing their photosynthesis. Compared to $KMnO_4$ alone, the removal of *H. akashiwo* cells was notably improved by the UV/$KMnO_4$ process. The algal cells could be completely removed by UV/$KMnO_4$ oxidation and the following self-settling process. Although humic acid inhibited the cell removal during UV/$KMnO_4$ oxidation and the initial 60 min of self-settling, the majority of algal cells could be efficiently removed during the followed self-settling time. The decrease in UV_{254} in the algal samples indicates that UV/$KMnO_4$ may mitigate the DBP formation potential and membrane fouling in the following water treatment processes. In addition, the build-up of hemolysis toxins can be avoided during the UV/$KMnO_4$ process. The UV/$KMnO_4$ process, which involves the use of a UV-lamp-equipped boat combined with the addition of $KMnO_4$, can be employed for the treatment of harmful algae in enclosed aquaculture systems. It can also be applied for pretreatment in seawater desalination and ship ballast water management systems to remove/inactivate harmful algae. Therefore, this study suggests that the UV/$KMnO_4$ process is an efficient alternative for controlling harmful marine algae in enclosed water.

Supplementary Materials: The following supporting information can be downloaded at: https://www.mdpi.com/article/10.3390/w15203633/s1, Table S1. Rate constants of $KMnO_4$ decay (k_{decay}) in the *H. akashiwo* samples treated with $KMnO_4$ and UV/$KMnO_4$ at dosages of 3, 5, and 7 mg L^{-1}. Figure S1. The water quality parameters of filtered algal culture treated with UV, $KMnO_4$ and UV/$KMnO_4$: (a) UV_{254} and (b) hemolysis rate. Conditions: $[KMnO_4]_0$ = 5 mg L^{-1}, exposure time = 0–30 min. Figure S2. The R_s of *H. akashiwo* samples during self-settling process after various treatments. Conditions: $[KMnO_4]_0$ = 5 mg L^{-1}, exposure time = 20 min.

Author Contributions: Conceptualization, X.C. and J.F.; Formal analysis, J.Z.; Investigation, J.Z.; Resources, J.F.; Data curation, J.Z. and S.J.; Writing—original draft, J.Z.; Writing—review & editing, J.F.; Visualization, J.Z.; Supervision, X.C. and J.F.; Project administration, J.F. All authors have read and agreed to the published version of the manuscript.

Funding: This research was supported by the National Natural Science Foundation of China (41730316 and 51708490) and the Scientific Research Foundation for Scholars of Hangzhou Normal University (2021QDL063).

Data Availability Statement: The data is available from the corresponding author upon request.

Acknowledgments: The authors thank the anonymous reviewers for their helpful comments and suggestions.

Conflicts of Interest: The authors declare no conflict of interest.

References

1. Griffith, A.W.; Gobler, C.J. Harmful algal blooms: A climate change co-stressor in marine and freshwater ecosystems. *Harmful Algae* **2020**, *91*, 101590. [CrossRef]
2. Wells, M.L.; Karlson, B.; Wulff, A.; Kudela, R.; Trick, C.; Asnaghi, V.; Berdalet, E.; Cochlan, W.; Davidson, K.; De Rijcke, M.; et al. Future HAB science: Directions and challenges in a changing climate. *Harmful Algae* **2020**, *91*, 101632. [CrossRef]
3. Basti, L.; Go, J.; Okano, S.; Higuchi, K.; Nagai, S.; Nagai, K. Sublethal and antioxidant effects of six ichthyotoxic algae on early-life stages of the Japanese pearl oyster. *Harmful Algae* **2021**, *103*, 102013. [CrossRef]

4. Sandoval-Sanhueza, A.; Aguilera-Belmonte, A.; Basti, L.; Figueroa, R.I.; Molinet, C.; Alvarez, G.; Oyanedel, S.; Riobo, P.; Mancilla-Gutierrez, G.; Diaz, P.A. Interactive effects of temperature and salinity on the growth and cytotoxicity of the fish-killing microalgal species *Heterosigma akashiwo* and *Pseudochattonella verruculosa*. *Mar. Pollut. Bull.* **2022**, *174*, 113234. [CrossRef]
5. Butrón, A.; Madariaga, I.; Orive, E. Tolerance to high irradiance levels as a determinant of the bloom-forming *Heterosigma akashiwo* success in estuarine waters in summer. *Estuar. Coast. Shelf Sci.* **2012**, *107*, 141–149. [CrossRef]
6. Butrón, A.; Orive, E.; Madariaga, I. Potential risk of harmful algae transport by ballast waters: The case of Bilbao Harbour. *Mar. Pollut. Bull.* **2011**, *62*, 747–757. [CrossRef]
7. Tobin, E.D.; Grunbaum, D.; Patterson, J.; Cattolico, R.A. Behavioral and physiological changes during benthic-pelagic transition in the harmful alga, *Heterosigma akashiwo*: Potential for rapid bloom formation. *PLoS ONE* **2013**, *8*, e76663. [CrossRef]
8. Caron, D.A.; Garneau, M.-È.; Seubert, E.; Howard, M.D.A.; Darjany, L.; Schnetzer, A.; Cetinić, I.; Filteau, G.; Lauri, P.; Jones, B.; et al. Harmful algae and their potential impacts on desalination operations off southern California. *Water Res.* **2010**, *44*, 385–416. [CrossRef]
9. Villacorte, L.O.; Tabatabai, S.A.A.; Dhakal, N.; Amy, G.; Schippers, J.C.; Kennedy, M.D. Algal blooms: An emerging threat to seawater reverse osmosis desalination. *Desalin. Water Treat.* **2014**, *55*, 2601–2611. [CrossRef]
10. Edzwald, J.K.; Haarhoff, J. Seawater pretreatment for reverse osmosis: Chemistry, contaminants, and coagulation. *Water Res.* **2011**, *45*, 5428–5440. [CrossRef]
11. Romero-Martinez, L.; Rivas-Zaballos, I.; Moreno-Andres, J.; Moreno-Garrido, I.; Acevedo-Merino, A.; Nebot, E. Effect of the length of dark storage following ultraviolet irradiation of *Tetraselmis suecica* and its implications for ballast water management. *Sci. Total Environ.* **2020**, *711*, 134611. [CrossRef] [PubMed]
12. Ou, H.; Gao, N.; Deng, Y.; Qiao, J.; Zhang, K.; Li, T.; Dong, L. Mechanistic studies of *Microcystic aeruginosa* inactivation and degradation by UV-C irradiation and chlorination with poly-synchronous analyses. *Desalination* **2011**, *272*, 107–119. [CrossRef]
13. Sinha, R.P.; Häder, D.-P. UV-induced DNA damage and repair: A review. *Photochem. Photobiol. Sci.* **2002**, *1*, 225–236. [CrossRef] [PubMed]
14. Jin, Y.; Chen, F.; Xu, B.; Ma, G.; Zhang, L.; Yang, Z.; Liu, R.; Sun, C.; Cheng, X.; Guo, N.; et al. Iron-based technology coupling moderate preoxidation with hybrid coagulation for highly effective removal and moderate growth inhibition of *Oscillatoria* in drinking water treatment plants. *J. Environ. Chem. Eng.* **2022**, *10*, 107723. [CrossRef]
15. Wang, H.; Yu, Z.; Cao, X.; Song, X. Fractal dimensions of flocs between clay particles and HAB organisms. *Chin. J. Oceanol. Limnol.* **2011**, *29*, 656–663. [CrossRef]
16. Chen, B.; Zeng, X.; Liu, X.; Ge, F.; Cheng, P. Coagulation performance and floc properties of *Microcystis aeruginosa* in the presence of humic acid. *Water Supply* **2015**, *15*, 339–347. [CrossRef]
17. Piezer, K.; Li, L.; Jeon, Y.; Kadudula, A.; Seo, Y. The application of potassium permanganate to treat cyanobacteria-laden water: A Review. *Process Saf. Environ.* **2021**, *148*, 400–414. [CrossRef]
18. Guo, K.; Zhang, J.; Li, A.; Xie, R.; Liang, Z.; Wang, A.; Ling, L.; Li, X.; Li, C.; Fang, J. Ultraviolet irradiation of permanganate enhanced the oxidation of micropollutants by producing HO• and reactive manganese species. *Environ. Sci. Technol. Lett.* **2018**, *5*, 750–756. [CrossRef]
19. Wei, W.; Guo, K.; Kang, X.; Zhang, J.; Li, C.; Fang, J. Complete removal of organoarsenic by the UV/Permanganate process via HO• oxidation and in situ-formed manganese dioxide adsorption. *ACS EST Eng.* **2021**, *1*, 794–803. [CrossRef]
20. Bai, M.; Zhang, Z.; Xue, X.; Yang, X.; Hua, L.; Fan, D. Killing effects of hydroxyl radical on algae and bacteria in ship's ballast water and on their cell morphology. *Plasma Chem. Plasma Process.* **2010**, *30*, 831–840. [CrossRef]
21. Chang, C.W.; Huo, X.; Lin, T.F. Exposure of *Microcystis aeruginosa* to hydrogen peroxide and titanium dioxide under visible light conditions: Modeling the impact of hydrogen peroxide and hydroxyl radical on cell rupture and microcystin degradation. *Water Res.* **2018**, *141*, 217–226. [CrossRef] [PubMed]
22. Petrusevski, V.; Van Breemen, A.; Alaerts, G. Effect of permanganate pre-treatment and coagulation with dual coagulants on algae removal in direct filtration. *J. Water Supply Res. Technol. AQUA* **1996**, *45*, 316–326.
23. Fan, J.; Zeng, J.; Li, X.; Guo, K.; Liu, W.; Fang, J. Multiple roles of UV/$KMnO_4$ in cyanobacteria containing water treatment: Cell inactivation & removal, and microcystin degradation. *J. Hazard. Mater.* **2023**, *457*, 131772. [CrossRef] [PubMed]
24. Henderson, R.; Parsons, S.A.; Jefferson, B. The impact of algal properties and pre-oxidation on solid–liquid separation of algae. *Water Res.* **2008**, *42*, 1827–1845. [CrossRef] [PubMed]
25. Wang, R.; Liu, Q. Responses of bloom-forming *Heterosigma akashiwo* to allelochemical linoleic acid: Growth inhibition, oxidative stress and apoptosis. *Front. Mar. Sci.* **2022**, *8*, 793567. [CrossRef]
26. Qu, F.; Du, X.; Liu, B.; He, J.; Ren, N.; Li, G.; Liang, H. Control of ultrafiltration membrane fouling caused by *Microcystis* cells with permanganate preoxidation: Significance of in situ formed manganese dioxide. *Chem. Eng. J.* **2015**, *279*, 56–65. [CrossRef]
27. Strock, J.S.; Menden-Deuer, S. Temperature acclimation alters phytoplankton growth and production rates. *Limnol. Oceanogr.* **2021**, *66*, 740–752. [CrossRef]
28. Markina, Z.V. The cell ultrastructure and autotrophic function of the raphidophyte alga *Heterosigma akashiwo* (Y. Hada) Y. Hada ex Y. Hara and M. Chihara, 1987 under Copper Exposure. *Russ. J. Mar. Biol.* **2021**, *47*, 204–209. [CrossRef]
29. Okamoto, T.; Kim, D.; Oda, T.; Matsuoka, K.; Ishimatsu, A.; Muramatsu, T. Concanavalin a-Induced discharge of glycocalyx of raphidophycean flagellates, *Chattonella marina* and *Heterosigma akashiwo*. *Biosci. Biotechnol. Biochem.* **2000**, *64*, 1767–1770. [CrossRef]

30. Jürgens, U.J.; Martin, C.; Weckesser, J. Cell wall constituents of *Microcystis* sp. PCC 7806. *FEMS Microbiol. Lett.* **1989**, *65*, 47–51. [CrossRef]
31. Saber, H.; El-Sheekh, M.M.; Ibrahim, A.; Alwaleed, E.A. Effect of UV-B radiation on amino acids profile, antioxidant enzymes and lipid peroxidation of some cyanobacteria and green algae. *Int. J. Radiat. Biol.* **2020**, *96*, 1192–1206. [CrossRef] [PubMed]
32. Wert, E.C.; Dong, M.M.; Rosario-Ortiz, F.L. Using digital flow cytometry to assess the degradation of three cyanobacteria species after oxidation processes. *Water Res.* **2013**, *47*, 3752–3761. [CrossRef] [PubMed]
33. Guillard, R.R.L. Culture of Phytoplankton for Feeding Marine Invertebrates. In *Culture of Marine Invertebrate Animals: Proceedings—1st Conference on Culture of Marine Invertebrate Animals Greenport*; Smith, W.L., Chanley, M.H., Eds.; Springer: Boston, MA, USA, 1975; pp. 29–60.
34. Rahn, R.O. Potassium iodide as a chemical actinometer for 254 nm radiation: Use of iodate as an electron scavenger. *Photochem. Photobiol.* **1997**, *66*, 885. [CrossRef]
35. Fan, J.; Rao, L.; Chiu, Y.-T.; Lin, T.-F. Impact of chlorine on the cell integrity and toxin release and degradation of colonial Microcystis. *Water Res.* **2016**, *102*, 394–404. [CrossRef]
36. Lin, S.; Yu, X.; Fang, J.; Fan, J. Influences of the micropollutant erythromycin on cyanobacteria treatment with potassium. *Water Res.* **2020**, *177*, 115786. [CrossRef]
37. Cheng, X.; Liang, H.; Ding, A.; Qu, F.; Shao, S.; Liu, B.; Wang, H.; Wu, D.; Li, G. Effects of pre-ozonation on the ultrafiltration of different natural organic matter (NOM) fractions: Membrane fouling mitigation, prediction and mechanism. *J. Membr. Sci.* **2016**, *505*, 15–25. [CrossRef]
38. Jeffrey, S.W.; Humphrey, G.F. New spectrophotometric equations for determining chlorophylls a, b, c1 and c2 in higher plants, algae and natural phytoplankton. *Plant Physiol. Biochem.* **1975**, *167*, 191–194. [CrossRef]
39. Strickland, J.; Parsons, T. A practical handbook of seawater analysis. *Bull. Fish. Res. Board Can.* **1968**, *167*, 185–194.
40. Chen, B.; Zhao, L.; Yu, Q.J. Toxicological effects of hypoxanthine on *Heterosigmaakashiwo*: Mechanism of growth inhibition and change in hemolytic toxin content. *Ecotox. Environ. Saf.* **2021**, *226*, 112797. [CrossRef]
41. Xu, H.; Pei, H.; Xiao, H.; Li, X.; Ma, C.; Hu, W. Inactivation of *Microcystis aeruginosa* by hydrogen-terminated porous Si wafer: Performance and mechanisms. *J. Photochem. Photobiol. Biol.* **2016**, *158*, 23–29. [CrossRef]
42. Bradford, M.M. A rapid and sensitive method for the quantitation of microgram quantities of protein utilizing the principle of protein-dye binding. *Anal. Biochem.* **1976**, *72*, 248–254. [CrossRef] [PubMed]
43. Fan, J.; Daly, R.; Hobson, P.; Ho, L.; Brookes, J. Impact of potassium permanganate on cyanobacterial cell integrity and toxin release and degradation. *Chemosphere* **2013**, *92*, 529–534. [CrossRef] [PubMed]
44. Ou, H.; Gao, N.; Deng, Y.; Qiao, J.; Wang, H. Immediate and long-term impacts of UV-C irradiation on photosynthetic capacity, survival and microcystin-LR release risk of *Microcystis aeruginosa*. *Water Res.* **2012**, *46*, 1241–1250. [CrossRef] [PubMed]
45. Ou, H.; Gao, N.; Wei, C.; Deng, Y.; Qiao, J. Immediate and long-term impacts of potassium permanganate on photosynthetic activity, survival and microcystin-LR release risk of *Microcystis aeruginosa*. *J. Hazard. Mater.* **2012**, *219–220*, 267–275. [CrossRef]
46. Yu, B.; Li, X.; He, M.; Li, Y.; Ding, J.; Zhong, Y.; Zhang, H. Selective production of singlet oxygen for harmful cyanobacteria inactivation and cyanotoxins degradation: Efficiency and mechanisms. *J. Hazard. Mater.* **2023**, *441*, 129940. [CrossRef]
47. Pathak, J.; Ahmed, H.; Singh, P.R.; Singh, S.P.; Häder, D.-P.; Sinha, R.P. Mechanisms of Photoprotection in Cyanobacteria. In *Cyanobacteria*; Mishra, A.K., Tiwari, D.N., Rai, A.N., Eds.; Academic Press: Cambridge, MA, USA, 2019; pp. 145–171.
48. Zhang, C.; Yi, Y.-L.; Hao, K.; Liu, G.-L.; Wang, G.-X. Algicidal activity of Salvia miltiorrhiza Bung on *Microcystis aeruginosa*—Towards identification of algicidal substance and determination of inhibition mechanism. *Chemosphere* **2013**, *93*, 997–1004. [CrossRef]
49. Li, D.; Cong, W.; Cai, Z.; Shi, D.; Ouyang, F. Some physiological and biochemical changes in marine eukaryotic red tide alga Heterosigma akashiwo during the alleviation from iron limitation. *Plant Physiol. Biochem.* **2003**, *41*, 295–301. [CrossRef]
50. Fan, G.; Bao, M.; Wang, B.; Wu, S.; Luo, L.; Li, B.; Lin, J. Inhibitory effects of Cu_2O/SiO_2 on the growth of *Microcystis aeruginosa* and Its mechanism. *Nanomaterials* **2019**, *9*, 1669. [CrossRef]
51. Mallick, N.; Mohn, F.H. Reactive oxygen species: Response of algal cells. *J. Plant Physiol.* **2000**, *157*, 183–193. [CrossRef]
52. Wang, W.; Liao, P.; Li, G.; Chen, H.; Cen, J.; Lu, S.; Wong, P.K.; An, T. Photocatalytic inactivation and destruction of harmful microalgae *Karenia mikimotoi* under visible-light irradiation: Insights into physiological response and toxicity assessment. *Environ. Res.* **2021**, *198*, 111295. [CrossRef]
53. Li, L.; Shao, C.; Lin, T.-F.; Shen, J.; Yu, S.; Shang, R.; Yin, D.; Zhang, K.; Gao, N. Kinetics of cell Inactivation, toxin release, and degradation during permanganation of *Microcystis aeruginosa*. *Environ. Sci. Technol.* **2014**, *48*, 2885–2892. [CrossRef]
54. Wang, L.; Qiao, J.; Hu, Y.; Wang, L.; Zhang, L.; Zhou, Q.; Gao, N. Pre-oxidation with $KMnO_4$ changes extra-cellular organic matter's secretion characteristics to improve algal removal by coagulation with a low dosage of polyaluminium chloride. *J. Environ. Sci. China* **2013**, *25*, 452–459. [CrossRef] [PubMed]
55. Hu, X.; Shi, L.; Zhang, D.; Zhao, X.; Huang, L. Accelerating the decomposition of $KMnO_4$ by photolysis and auto-catalysis: A green approach to synthesize a layered birnessite-type MnO_2 assembled hierarchical nanostructure. *RSC Adv.* **2016**, *6*, 14192–14198. [CrossRef]
56. Park, K.Y.; Choi, S.Y.; Ahn, S.K.; Kweon, J.H. Disinfection by-product formation potential of algogenic organic matter from *Microcystis aeruginosa*: Effects of growth phases and powdered activated carbon adsorption. *J. Hazard. Mater.* **2021**, *408*, 124864. [CrossRef] [PubMed]

57. Qi, J.; Lan, H.; Liu, R.; Liu, H.; Qu, J. Fe(II)-regulated moderate pre-oxidation of *Microcystis aeruginosa* and formation of size-controlled algae flocs for efficient flotation of algae cell and organic matter. *Water Res.* **2018**, *137*, 57–63. [CrossRef] [PubMed]
58. Chen, J.; Rao, D.; Dong, H.; Sun, B.; Shao, B.; Cao, G.; Guan, X. The role of active manganese species and free radicals in permanganate/bisulfite process. *J. Hazard. Mater.* **2020**, *388*, 121735. [CrossRef] [PubMed]
59. Minakata, D.; Crittenden, J. Linear free energy relationships between aqueous phase hydroxyl radical reaction rate constants and free energy of activation. *Environ. Sci. Technol.* **2011**, *45*, 3479–3486. [CrossRef]
60. Ling, C.; Trick, C.G. Expression and standardized measurement of hemolytic activity in *Heterosigma akashiwo*. *Harmful Algae* **2010**, *9*, 522–529. [CrossRef]
61. Zhu, Q.; Wu, B.; Zhao, L. Effect of algicidal compound Nomega-acetylhistamine on physiological response and algal toxins in *Heterosigma akashiwo*. *Ecotoxicol. Environ. Saf.* **2021**, *208*, 111423. [CrossRef]
62. Enriquez, R.; Pichat, P. Interactions of humic acid, quinoline, and TiO_2 in water in relation to quinoline photocatalytic removal. *Langmuir* **2001**, *17*, 6132–6137. [CrossRef]
63. Westerhoff, P.; Aiken, G.; Amy, G.; Debroux, J. Relationships between the structure of natural organic matter and its reactivity towards molecular ozone and hydroxyl radicals. *Water Res.* **1999**, *33*, 2265–2276. [CrossRef]
64. Chen, J.J.; Yeh, H.H. The mechanisms of potassium permanganate on algae removal. *Water Res.* **2005**, *39*, 4420–4428. [CrossRef] [PubMed]
65. Zhang, X.; Xu, W.; Ren, P.; Li, W.; Yang, X.; Zhou, J.; Li, J.; Li, Z.; Wang, D. Effective removal of diatoms (*Synedra* sp.) by pilot-scale UV/chlorine-flocculation process. *Sep. Purif. Technol.* **2022**, *302*, 122117. [CrossRef]
66. Liu, R.; Liu, H.; Qiang, Z.; Qu, J.; Li, G.; Wang, D. Effects of calcium ions on surface characteristics and adsorptive properties of hydrous manganese dioxide. *J. Colloid Interface Sci.* **2009**, *331*, 275–280. [CrossRef]
67. Pilson, M.E.Q. *An Introduction to the Chemistry of the Sea*, 2nd ed.; Cambridge University Press: Cambridge, UK, 2012.